HHS Public Access

Author manuscript

*Cell Mol Neurobiol*. Author manuscript; available in PMC 2019 May 01.

Published in final edited form as:

*Cell Mol Neurobiol*. 2018 May ; 38(4): 941–954. doi:10.1007/s10571-017-0568-z.

# The Ferroxidase Hephaestin But Not Amyloid Precursor Protein is Required for Ferroportin-Supported Iron Efflux in Primary Hippocampal Neurons

**Changyi Ji**[1], **Brittany L. Steimle**[1], **Danielle K. Bailey**[1], and **Daniel J. Kosman**[1,2,iD]

[1]Department of Biochemistry, School of Medicine and Biomedical Sciences Buffalo, State University of New York, New York, NY 14214, USA

[2]Department of Biochemistry, The University at Buffalo, Farber Hall Room 140, 3435 Main St, Buffalo, NY 14214-3000, USA

## Abstract

Iron efflux in mammalian cells is mediated by the ferrous iron exporter ferroportin (Fpn); Fpn plasma membrane localization and function are supported by a multicopper ferroxidase and/or the soluble amyloid precursor protein (sAPP). Fpn and APP are ubiquitously expressed in all cell types in the central nervous system including neurons. In contrast, neuronal ferroxidase(s) expression has not been well characterized. Using primary cultures of hippocampal neurons, we examined the molecular mechanism of neuronal Fe efflux in detail. Developmental increases of Fpn, APP, and the ferroxidase hephaestin (Hp) were observed in hippocampal neurons. Iron efflux in these neurons depended on the level of Fpn localized at the cell surface; as noted, Fpn stability is supported by ferroxidase activity, an enzymatic activity that is required for Fe efflux. Iron accumulation increases and iron efflux decreases in Hp knockout neurons. In contrast, suppression of endogenous APP by RNAi knockdown does not affect surface Fpn stability or Fe efflux. These data support the model that the neuronal ferroxidase Hp plays a unique role in support of Fpn-mediated Fe efflux in primary hippocampal neurons. Our data also demonstrate that Hp ferroxidase activity relies on copper bioavailability, which suggests neuronal iron homeostasis will be modulated by cellular copper status.

Correspondence to: Danielle K. Bailey.

Daniel J. Kosman http://orcid.org/0000-0003-3570-7682

Electronic supplementary material The online version of this article (https://doi.org/10.1007/s10571-017-0568-z) contains supplementary material, which is available to authorized users.

**Author Contributions** Changyi Ji and Daniel J. Kosman designed the study, analyzed the data, and wrote the paper. Changyi Ji, Brittany Steimle, and Danielle Bailey performed the experiments.

**Compliance with Ethical Standards**

**Ethical Approval** All contributors to this manuscript have participated in the Ethical Standards and Scientific Integrity program conducted by the Vice President of Research at the University at Buffalo.

**Research Involved in Animal Rights** All applicable international, national, and institutional guidelines for the care and use of animals were followed. All procedures performed in studies involving animals were in accordance with the ethical standards of the State University of New York. The use of animals in this research was approved and supervised by the Animal Care and Use Committee and the Division of Comparative Medicine and Laboratory Animal Facilities in the Jacobs School of Medicine and Biomedical Sciences, The University at Buffalo.

**Conflict of interest** The authors declare that they have no competing interests.

**Keywords**

Primary hippocampal neurons; Iron efflux; Ferroportin (Fpn); Hephaestin (Hp); Amyloid precursor protein (APP); Ferroxidase

## Introduction

Iron is an essential co-factor for enzymes involved in a variety of normal neuronal functions (Altamura and Muckenthaler 2009). Insufficient iron impairs neuronal development (Greminger et al. 2014; Matak et al. 2016; Breton et al. 2015), while brain iron accumulation is associated with aging and neurodegeneration (Ghadery et al. 2015; Dexter et al. 1991). Such neurological disorders include Alzheimer's and Parkinson's diseases (Smith et al. 1997; Dexter et al. 1987). To support normal neuronal function, iron homeostasis needs to be tightly regulated.

Iron efflux plays an important role in maintaining neuronal iron homeostasis. This process is mediated by the only known mammalian iron exporter ferroportin (Fpn) (Abboud and Haile 2000) and a ferroxidase such as ceruloplasmin (Cp), hephaestin (Hp), or zyklopen (Zp) (Jeong and David 2003; Chen et al. 2004, 2010). Cp, Hp, and, perhaps, Zp stabilize Fpn on the cell surface through a mechanism that likely relies on their physical interaction. This interaction is indicated by the co-immunoprecipitation of Fpn and soluble Cp (sCp) (McCarthy and Kosman 2014; Wong et al. 2014), glycosylphosphatidylinositol-anchored Cp (GPI-Cp) (De Domenico et al. 2007; Jeong and David 2003), and Hp (Yeh et al. 2011) with Fpn. The presence of ferroxidase activity also increases surface Fpn stability (De Domenico et al. 2007; Jeong and David 2003) and promotes Fe efflux by catalyzing ferrous iron oxidation. Multicopper ferroxidases use copper ions as cofactors to catalyze the four-electron reduction of dioxygen to two $H_2O$; this dioxygen reduction is supported by the oxidation of four $Fe^{2+}$ ions to the ferric iron valence state.

The absence of ferroxidase or its activity affects iron efflux and causes iron accumulation in neuroglia including astrocytes and oligodendrocytes (Jeong and David 2003, 2006; Schulz et al. 2011). Cp knockout mice demonstrate age-related iron accumulation, which is mainly observed in cerebellar astrocytes (Jeong and David 2006). Patients with aceruloplasminemia exhibit a low level of functional Cp and brain iron accumulation, and also develop progressive neurologic dysfunction (Melgari et al. 2015; Vroegindeweij et al. 2015). Compared to Cp knockout mice, Hp mutant or knockout mice exhibit an earlier onset of brain iron accumulation as well as motor deficits (Jiang et al. 2015; Schulz et al. 2011); iron is accumulated in cortex, hippocampus, brain stem, and cerebellum in these mice (Jiang et al. 2015). Although these genetically modified mice exhibit neurodegeneration, the neuronal iron status has not been specifically addressed. Moreover, the molecular mechanisms of neuronal iron efflux remain to be elucidated.

Neurons express Fpn (Wu et al. 2004; Moos and Rosengren Nielsen 2006; Boserup et al. 2011; Aguirre et al. 2005) and Fpn expression increases during brain development in the postnatal rat brain (Moos and Rosengren Nielsen 2006). Membrane attached GPI-Cp is predominantly expressed in astrocytes (Jeong and David 2003), while sCp is found in

cerebrospinal fluid (Olivieri et al. 2011; Barbariga et al. 2015). Hp is broadly expressed in a variety of brain cells, including microvascular endothelial cells, oligodendrocytes, and nigral neurons (Schulz et al. 2011; Song et al. 2010b; McCarthy and Kosman 2013). The different expression patterns for Hp and Cp suggest non-redundant roles in modulating iron efflux in different neural cell populations.

β-Amyloid precursor protein (APP) is ubiquitously expressed in the brain (Apelt et al. 1997). A role for APP in neuronal iron efflux was first suggested by Bush and co-workers. The underlying mechanism was attributed to a proposed ferroxidase activity of APP which was hypothesized to support Fpn-mediated neuronal iron efflux (Duce et al. 2010). Subsequent reports from other groups demonstrated that APP had no ferroxidase activity (Honarmand Ebrahimi et al. 2013; McCarthy et al. 2014). However, direct interaction between APP and Fpn at the cell surface was shown to promote surface Fpn stability and thereby contributed to iron efflux in the presence of a ferroxidase (McCarthy et al. 2014; Wong et al. 2014; Duce et al. 2010). Endogenous APP is coimmunoprecipitated with Fpn; exogenous APP is associated with surface Fpn in cortical neurons (Duce et al. 2010). This interaction is required for Fpn surface trafficking in a neuronal cell line (Wong et al. 2014). As has been demonstrated in brain microvascular endothelial cells, sAPPα increased Fpn stability when endogenous Hp was depleted; however, iron efflux was stimulated only when Cp or the yeast ferroxidase homolog, Fet3p, was present (McCarthy et al. 2014). Therefore, the role of APP in neuronal iron efflux needs to be re-evaluated if an endogenous ferroxidase is expressed in neurons.

In this paper, we dissected the molecular mechanism of neuronal iron efflux using primary hippocampal neurons as an in vitro model. We have shown that hippocampal neurons express Hp. The surface Fpn and Hp abundance is developmentally regulated in a pattern that correlates with Fe efflux from these neurons. In the absence of Hp, hippocampal neurons accumulate more iron and have less iron efflux. In contrast, knockdown of the expression of endogenous APP does not affect surface Fpn abundance nor iron efflux from these cells. Neuronal ferroxidase activity is regulated by copper bioavailability which, therefore, modulates surface Fpn stability and subsequent iron efflux. Thus, Hp is a key ferroxidase that plays a direct role in Fpn-mediated Fe efflux in hippocampal neurons.

## Methods

### Animals

Timed pregnant female Sprague Dawley rats were purchased from Envigo (Indianapolis, IN). The C57BL/6J wild-type female mice were obtained from Jackson Laboratory (Stock No: 000664, Bar Harbor, ME), and *HEPH* full knockout male mouse on C57BL/6J background was kindly provided by Professor Joshua Dunaief at the University of Pennsylvania. The *HEPH* knockout and wild-type mice breeding pairs were generated and maintained in the animal facility at University at Buffalo. All mice had access to an unlimited standard rodent chow diet and water. All procedures were handled in accordance with and approval by the Institutional Animal Care and Use Committee of the University at Buffalo.

## Primary Hippocampal Neuronal Culture

Primary rat hippocampal neurons were prepared from D18 or D19 Sprague Dawley rat embryos as previous described (Ji and Kosman 2015). Primary mouse hippocampal neurons were prepared from D0 postnatal mouse pups as previously described (Beaudoin et al. 2012). Neurons were plated at a density of $1.5 \times 10^5$ cells on poly-D-lysine-coated cover-slips for immunofluorescence studies, a moderate density of $2 \times 10^5$ cells/well in coated 12-well plates for $^{59}$Fe-efflux assays, or a high density of $2–3 \times 10^6$ cells in 6-cm coated dishes for biotinylation, protein, and oxidase activity assays. Coated culture dishes were obtained from Corning (Corning, NY). Cells were maintained in Neurobasal media supplemented with B27 and L-glutamine (Gibco/Thermo Fisher Scientific, Grand Island, NY). On day 3 post-plating, AraC (Sigma-Aldrich, St. Louis, MO) was added to inhibit the proliferation of glial cells. The concentrations of these two additions were as follows: for mouse neurons, 5 μM for each; for rat neurons, 0.5 μM and 2 μM, respectively. Thereafter, one-third of the medium was replaced every 4 days. Using this method, both rat and mouse hippocampal neurons were grown in culture for up to 21 days during which time they exhibited extensive outgrowth of branching processes; no difference in this growth pattern was observed between wild-type rat and Hp KO mouse neurons, nor was any change in this cell morphology visualized during the iron loading and efflux time course. Nearly pure primary neuronal cultures were used in these experiments (~ 98% pure) as indicated by the immunostaining of MAP2 as a neuronal marker in comparison to the lack of detectable GFAP staining as a glial marker (Ji and Kosman 2015). Neurons were used between D11 and D20 post-plating as indicated.

## Treatments

Copper depletion was achieved by treating hippocampal neurons with 1 μM ammonium tetrathiomolybdate (TTM) (Sigma-Aldrich, St. Louis, MO) and 200 μM bathocuproine disulfonate (BCS) (Sigma-Aldrich, St. Louis, MO) together for 48 h at 37 °C. Equal volume of double-distilled water was added in control treatments.

## Genomic DNA Isolation and PCR

Genomic DNA was isolated from mouse neurons growing for 12 days in culture using Omega E.Z.N.A.® Tissue DNA Kit (Omega Bio-Tek, Norcross, GA) as per the manufacturer's instructions. Genotyping PCR followed the protocol described in (Wolkow et al. 2012). For detecting the wild-type allele, the primers used were forward, 5′-CTTTGGACCACACATGCAAC-3′ and reverse, 5′-AAAACCCAGCTCCTCCATTT-3′. The annealing temperature was 52 °C. The expected size for the wild-type allele was 564 bp. For detecting the *HEPH* knockout allele, the primers used were forward, 5′-GACAAGAGCTCTAGGAGAGATGCCA-3′ and reverse, 5′-CCAAGCATTCAGTAGACCTAGGAAGGA-3′. The annealing temperature was 58.5 °C. The expected band size for the *HEPH* knockout allele was 363 bp.

## RT-PCR and Quantitative RT-PCR

Total RNA was prepared by lysing neurons in TRIzol reagent (Thermo Fisher Scientific, Waltham, MA), followed by RNA extraction and clean-up using the Directzol RNA

MiniPrep kit (Zymo Research, Irvine, CA) following the manufacturer's protocol. One-step RT-PCR was performed using the QIAGEN®One-Step RT-PCR Kit (Qiagen, Hilden, Germany) and analyzed on 2% agarose gels. Primers using for detecting mRNA of each protein were as follows: Fpn, forward, 5′-CAGGGACTGAGTGGTTCCAT-3′, reverse, 5′-GGAGATTATGGGGACGGATT-3′; Hp, forward, 5′-GGATGCATGCAATCAATGG-3′, reverse, 5′-CATCTTGAAAGGCTTCATATCG-3′; GPI-Cp, forward, 5′-GTATGTGATGGCTATGGGCAATGA-3′, reverse, 5′-CCTGGATGGAACTGGTGATGGA-3′; and sCp, forward, 5′-TCCACTGCCATGTGACTGAC-3′, reverse, 5′-TCGGCATTACCAATTCCCTCA-3′. Quantitative RT-PCR was performed following a two-step protocol. First-strand cDNA was synthesized from 0.5 μg total RNA by using the iScript™ cDNA synthesis kit (Bio-Rad Laboratories, Hercules, CA). Real-time PCRs were performed using SsoAdvanced™ universal supermixes (Bio-Rad Laboratories, Hercules, CA) on a CFX96 Touch™ Real-Time PCR Detection System (Bio-Rad Laboratories, Hercules, CA). Primers recognizing *HEPH* exon 4, the region targeted for deletion, were used as described (Wolkow et al. 2012). Primers used for TfR1 were forward, 5′-GAATAAATTCCCCGTTGTTGA-3′, reverse, 5′-ATCACCAGTTCCTAGATGAGCAT-3′. Relative expression of target mRNA was normalized to β-actin as a housekeeping control and calculated as $\Delta\Delta C_t$.

## Surface Protein Biotinylation

Neurons growing in high density were cooled on ice for 5 min and washed twice with ice-cold PBS containing 1 mM $CaCl_2$ and 0.5 mM $MgCl_2$ (PBS/Ca/Mg). The cultures were treated with EZ-Link Sulfo-NHS-SS-biotin (1 mg/ml, Thermo Fisher Scientific, Waltham, MA) for 30 min at 4 °C. Biotinylation was stopped by washing cells with 0.1% BSA in PBS/Ca/Mg twice followed by two additional washes with PBS/Ca/Mg alone. Cells were scraped into ice-cold RIPA buffer (50 mM Tris, 150 mM NaCl, 1 mM EDTA, 1% Triton X-100, 0.5% Na-deoxycholate, 0.5% SDS, pH 7.4) containing a cocktail of broad-spectrum protease inhibitors (Thermo Fisher Scientific, Waltham, MA). Cell lysates were incubated on ice for 15 min, then clarified by centrifugation at 13,000×*g* for 10 min. Supernatant protein concentration was measured by BCA assay (Thermo Fisher Scientific, Waltham, MA). Lysates (300 μg total protein) were incubated with 200 μl NeutrAvidin agarose (Thermo Fisher Scientific, Waltham, MA) at 4 °C overnight. Intracellular protein was separated as the unbound fraction. After thoroughly washing the column, the bound, surface protein fraction was recovered from the agarose by 30 min incubation at 50 °C in SDS-loading buffer containing DTT (Thermo Fisher Scientific, Waltham, MA).

## Western Blots

Total protein (20–30 μg) was resolved in 4–15% Tris-Glycine SDS-polyacrylamide gel (Bio-Rad Laboratories, Hercules, CA), and then transferred to a nitrocellulose or PVDF membrane. Membranes were blocked by TBST (Tris-buffered saline with 0.1% Tween-20) containing 5% BSA at 22 °C for 1 h. Primary antibodies were diluted in 1% BSA-TBST as follows: 1:10,000 for rabbit anti-Fpn (Abcam, ab85370) and mouse anti-APP (Millipore, 22C11); 1:5000 for mouse anti-Hp (Abcam, ab56729), rabbit anti-β-actin (Cell Signaling, 13E5), and goat anti-Na–K-ATPase (Santa Cruz Biotechnology, C16), then incubated with membranes at 4 °C overnight. After wash, membranes were incubated for 1 h at 22 °C with

the cognate HRP-conjugated secondary goat anti-mouse, goat anti-rabbit, or donkey anti-goat antibody diluted in TBST containing 3% BSA (Santa Cruz Biotechnology). The immunoblot was developed using SuperSignal West Dura Extended Duration Substrate (Thermo Scientific, Waltham, MA) and band intensity was quantified in Image Studio Lite (Licor Biosciences, Lincoln, NE).

### $^{59}$Fe Accumulation and Efflux

$^{59}FeCl_3$ (1 μM, Perkin Elmer, Waltham, MA) complexed with 4 μM NTA was incubated with neurons in complete Neurobasal medium for 16 h at 37 °C. After $^{59}$Fe loading, cells were washed thoroughly with DMEM medium containing 20 mM HEPES (pH 7.4) and 1 mM citrate. A set of neurons, counted as "$t = 0$" or total-accumulated $^{59}$Fe, were lysed; fresh efflux medium (DMEM medium containing 20 mM HEPES) was added to another set of neurons, which were then incubated at 37 °C. An aliquot of medium was removed from these cultures every 2 h over a 6-h efflux period. $^{59}$Fe efflux was terminated by washing cells twice with an ice-cold EDTA-containing quench buffer. These $t = 6$ h cells were lysed. Both medium- and cell-associated $^{59}$Fe were quantified using an LKB Wallac CompuGamma instrument. The quantity of $^{59}$Fe was normalized to total protein in each sample as determined by BCA assay.

### In-gel *p*-phenylenediamine (pPD) Oxidase Assay

An in-gel *p*-phenylenediamine (pPD) assay was performed under non-denaturing and non-reducing conditions as described (Chen et al. 2010, 2006, 2004). Briefly, neurons were lysed in PBS containing 1% Triton X-100 (PBST, pH 7.4) and a protease inhibitor cocktail (Thermo Fisher Scientific, Waltham, MA). The protein sample (80–100 μg) was mixed with native sample buffer lacking DTT and electrophoretically resolved in a 4–12% Tris-Glycine native-PAGE gel (Thermo Fisher Scientific, Grand Island, NY) without prior heating. The gels were incubated for 2 h in a 0.1% pPD in 0.1 mol/L acetate buffer (pH 5.45). Amine oxidase activity was indicated by accumulation of a purple chromogen as gels were air-dried in the dark. Color development was monitored by scanning and quantified in Image Studio Lite (Licor Biosciences, Lincoln, Nebraska). The experimental protocols were repeated three times as were the gel assays for each biologic replicate (technical replicates). A representative chromogram is shown.

### Lentiviral-mediated Short-hairpin RNA (shRNA) Knockdown

A lentiviral system was used to deliver short-hairpin RNA (shRNA) into hippocampal neurons as previous described (Ji and Kosman 2015). A validated APP targeting sequence used previously in siRNA APP knockdown (Young-Pearse et al. 2007) was adapted for cloning into the pLKO.3G lentiviral vector (Addgene). Lentivirus particles were produced in HEK293T/17 cells. Particle-containing medium was concentrated by ultracentrifugation and re-suspended in fresh Neurobasal medium. Primary rat hippocampal neurons were infected at day 2 post-plating at an MOI of 20 in a halfvolume of culture medium. After 24 h, the virus-containing medium was removed and fresh full Neurobasal medium supplemented with half-conditioned medium containing 2 μM AraC was added back. Neurons were maintained until day 14 post-plating. The efficiency of APP protein knockdown was

confirmed by western blotting, followed by surface biotinylation or $^{59}$Fe assays as described above.

### Statistical Analysis

Data are presented as mean ± SD. Technical replicates, referred to "*n*=," and experimental (biologic) replicates are given in each figure. Statistical analyses were performed using GraphPad Prism 6 (GraphPad Software, San Diego, CA, USA). Statistical significance was tested by either unpaired t-test, or one-way ANOVA followed by Bonferroni pair-wise comparison *post hoc* test, or two-way ANOVA with Sidak's multiple comparisons test, as noted.

## Results

### Developmental Changes in Expression of Fe-efflux Proteins and $^{59}$Fe Efflux in Primary Hippocampal Neurons

Primary hippocampal neurons were used as an in vitro cell model which allows us to perform kinetic analysis of neuronal iron efflux. First, we examined the expression of proteins associated with iron efflux in these neurons. Fpn and Hp transcripts were both detected (Fig. 1a). The expression of Fpn and Hp at the protein level was also observed (Fig. 1b). Although GPI-linked Cp and sCp were found at the mRNA level, neither was detectable at the protein level in the hippocampal neuronal lysate or conditioned medium (Fig. s1). Consistent with previous reports, APP protein was detected in lysates (Fig. 1b). The expression patterns of Fpn, APP, and Hp in developing neuronal culture were also investigated. Fpn expression was observed throughout neuronal development with no significant change from DIV11 to DIV20 (Fig. 1b). APP expression increased in this time period; both immature and mature forms exhibited a change (Fig. 1b). The protein pattern illustrated in this western blot represents the different glycosylated APP species found in neurons (Lei et al. 2012). A higher molecular weight Hp species increased in abundance while the lower molecular weight form did not (Fig. 1b). The higher molecular bands represent N-glycosylated Hp (Fig. s2).

The abundance of Fe-efflux proteins on the plasma membrane controls the level of Fe efflux. Thus, the presence of these proteins localized on the cell surface was assessed in the developing neurons. The surface Fpn moderately increased from DIV11 to DIV15, and remained constant up to DIV20 (Fig. 1b, c). Similarly, the surface APP increased from DIV11 to DIV20; notably, only the mature APP form was detected on the neuronal cell surface as expected (Fig. 1b, c). Interestingly, a dramatic increase of surface Hp was observed from DIV11 to DIV20 (Fig. 1b, c). The presence of Fe-efflux proteins at the cell surface constitutes the molecular basis for Fe efflux in primary hippocampal neurons. These increases of surface Fpn, Hp, and APP would support a more robust Fe efflux in mature neurons in comparison to immature ones.

To test this hypothesis, neurons of increasing maturity were loaded with 1 μM $^{59}$Fe and then assayed for $^{59}$Fe efflux. More $^{59}$Fe was observed in the medium of D20 neurons in comparison to those in culture for 15 and 11 days, respectively (Fig. 2a). Linear regression

analysis of the Fe efflux provided velocities of Fe efflux, which were then replotted versus the days in culture (development). These data showed that Fe efflux increased from DIV11 to DIV20 (Fig. 2b) a pattern that correlated with the increase of surface Fpn, Hp, and APP.

## APP does not Contribute to $^{59}$Fe efflux in Primary Hippocampal Neurons

The role of endogenous APP in stabilizing surface Fpn and Fe efflux was examined in these neurons. To do so, endogenous APP was suppressed by shRNA delivered *via* lentivirus (Fig. 3a, b). A significant knockdown of APP in primary hippocampal neurons was observed. However, surface Fpn did not change significantly in the absence of surface APP (Fig. 3c). In addition, surface Hp appeared to increase slightly in the absence of APP, and decrease in the presence of sAPP added exogenously (Fig. 3c). The quantification of surface Fpn, APP, and Hp is summarized in Fig. 3d. Neurons did not accumulate more $^{59}$Fe in the absence of endogenous APP as would be expected if iron efflux were, in part, dependent on expression of this protein; also, the level of cell-associated $^{59}$Fe was not changed by addition of exogenous sAPP (Fig. 4a). Last, knockdown of APP had no effect on $^{59}$Fe efflux (Fig. 4b). In summary, the data indicate that endogenous APP is dispensable with respect to maintenance of surface Fpn and Fe efflux in hippocampal neurons.

## Neuronal Ferroxidase Hp is Required for $^{59}$Fe Efflux in Primary Hippocampal Neurons

Ferroxidases play dual roles in iron efflux: they stabilize surface Fpn while catalyzing Fe oxidation to facilitate the Fe efflux from Fpn (De Domenico et al. 2007). Endogenously expressed Hp is a likely candidate that supports the ferroxidase activity in these neurons. To test this hypothesis, primary hippocampal neurons isolated from wild-type or *Hp* knockout mice were prepared and genotyped (Fig. 5a). In *Hp* knockout mice, deletion of *Hp* exon4, which encodes the trinuclear copper cluster required for ferroxidase activity, introduces an early stop codon and causes the remaining coding sequence to be out of frame (Wolkow et al. 2012). Quantitative RT-PCR was performed to confirm the absence of exon 4 region in Hp transcripts isolated from Hp knockout neurons (Fig. 5b). The absence of full-length Hp expression was also demonstrated by a western blot (Fig. 5c). Genetic disruption of *Hp* alters cellular ferroxidase activity (Chen et al. 2004). As demonstrated in the in-gel *p*-phenylenediamine oxidase activity assay, wild-type neuronal lysates exhibited robust oxidase activity, whereas this activity decreased in Hp knockout neuronal lysates; sCp and a Caco-2 lysate were used as positive controls (Fig. 5d). Hp knockout neurons had a decreased abundance of transferrin receptor (TfR) transcripts (Fig.s3). However, more $^{59}$Fe was accumulated in Hp knockout neurons compared to the wild-type neurons (Fig. 5e). The presence of exogenous ferroxidase sCp partially decreased $^{59}$Fe accumulation in Hp knockout neurons (Fig. 5e). These observations suggested the increase of $^{59}$Fe retention is attributable to a decreased ability of Fe efflux rather than an increase of Fe uptake in Hp knockout neurons. We further tested this prediction in a $^{59}$Fe-efflux assay. There was a decrease in the loss of cellassociated $^{59}$Fe in Hp knockout neurons compared to wild type (Fig. 5f), in support of the premise that Hp contributes to neuronal iron efflux.

We further investigated the functional role of Hp as a ferroxidase in neuronal Fe efflux. As has been well-documented, cell multicopper ferroxidase activity is inhibited by Cu chelators, e.g., ammonium tetrathiomolybdate (TTM) and bathocuproine disulfonate (BCS) (Chen et

al. 2006; McCarthy and Kosman 2013; Chidambaram et al. 1984). We observed a reduction of oxidase activity in primary neuronal cultures treated with TTM/BCS for 48 h, an inhibition that persisted for up to 90 h (Fig. 6a, b). To test if this suppression of neuronal oxidase activity affected Fe efflux in these cells, we first examined surface protein expression in the absence or presence of Cu chelation. Surface Fpn significantly decreased in the neurons treated with TTM/BCS for 48 h in comparison to control cells (Fig. 6c, d); surprisingly, surface Hp did not change, nor did surface APP (Fig. 6c, d). However, this Cu chelation and resulting decrease in surface Fpn correlated with significant $^{59}$Fe accumulation (Fig. 7a) and impaired $^{59}$Fe efflux (Fig. 7d). More $^{59}$Fe was associated with cell pellets and less $^{59}$Fe was present in the medium in the TTM/BCS-treated cultures (Fig. 7c). To further confirm, ferroxidase activity is required for Fe efflux in primary hippocampal neurons, sCp was added back to the neuronal culture treated with TTM/BCS. In the presence of this exogenous sCp, the Cu-limited neuronal cultures did not accumulate the excess $^{59}$Fe seen in these cells in the absence of this added sCp (Fig. 7d). In summary, these data support the conclusion that in hippocampal neurons ferroxidase activity supported by endogenous Hp has a direct impact on Fpn membrane localization and on the subsequent iron efflux through this ferrous iron transporter. Copper availability in these neurons affects Hp ferroxidase activity and consequentially modulates iron efflux in these cells.

## Discussion

Iron efflux depends on the presence of the iron exporter, Fpn, and its partner ferroxidase(s) (Jeong and David 2003; McCarthy and Kosman 2013). Loss of ferroxidase protein and activity leads to iron accumulation in neural tissues (Jeong and David 2006; Jiang et al. 2015; Chen et al. 2004; Schulz et al. 2011). In this report, we used primary neurons isolated from the mouse and rat hippocampus to identify the neuronal ferroxidase Hp and investigate its role in Fpn supported iron efflux. Our data demonstrate that in the absence of Hp or its ferroxidase activity, Fpn-mediated Fe efflux in these neurons is markedly reduced which leads to an increase in intracellular iron level. A reduction in TfR transcript abundance in Hp knockout neurons may represent a secondary response to the elevated intracellular level via the canonical IRP/IRE regulatory mechanism.

The expression pattern of iron efflux-related proteins in primary hippocampal neurons is consistent with previous observations. First, Fpn mRNA and protein in nearly pure primary hippocampal neurons were observed, which confirms that Fe efflux from primary hippocampal neurons depends on this unique mammalian iron exporter (Wu et al. 2004; Moos and Rosengren Nielsen 2006). Hp expression has been reported in nigral neurons (Song et al. 2010a), and its down-regulation is implicated in iron accumulation in Parkinson’s disease models (Wang et al. 2007). In addition to these observations, Hp expression in hippocampal neurons suggests the possible involvement of this ferroxidase in iron efflux in these neurons. Although GPI-Cp and sCp transcripts were detected, these species could not be detected at the protein level. One possible source of the Cp mRNA indicated by our data is a residual glial cell population (~1%); also, the abundance of Cp protein expressed could be below the detection limit in the western blots. APP protein, as expected, was expressed in our cultured neurons.

Developmental increases of iron efflux-related proteins have been reported in several *in vivo* studies. Fpn immunoreactivity has been observed in neurons at all developmental stages with the highest level found at postnatal day 21, particularly in axons and white matter tracts (Moos and Rosengren Nielsen 2006). An increase of Hp expression has been observed in rat brains from postnatal week 1 to week 28 (Qian et al. 2007). APP transcripts are present in rat brains throughout development (Apelt et al. 1997). By collecting lysates from neurons at different stages of development *in vitro*, we were able to recapitulate the developmental patterns noted for Fpn, Hp, and APP during the neuronal maturation process *in vivo*. Cultures at D11, D15, and D20, time points that are equivalent to postnatal days 8, 12, and 17, were chosen for this study. During this time period, neuronal dendritic processes branch out, which is concurrent with synaptogenesis (Baj et al. 2014). Neurons are considered mature after D14 in vitro (Baj et al. 2014). From D11 to D20 in these neurons, changes in the total amount of Fpn, APP, or Hp are not prominent; however, the abundances of surface Fpn, APP, and especially Hp significantly increase. More surface-localized Fpn supports robust increase of iron efflux in these more mature neurons, as measured by our assays. This is the advantage of using an *in vitro* culture, which allows for the quantification of neuronal iron efflux as a function of the expression of the proteins and their activities that support this iron trafficking.

APP and Hp interact with Fpn on the cell surface (McCarthy et al. 2014; Wong et al. 2014; Duce et al. 2010). In addition to this interaction, Hp possesses ferroxidase activity, which is also important in support of the surface Fpn stability (Chen et al. 2004). Previous studies have indicated that iron is accumulated in APP knockout neurons, a phenotype that was attributed to less iron efflux in these neurons compared to the controls (Duce et al. 2010). Similar observations have been made in APP-silenced HEK (Duce et al. 2010) and neuroblastoma SH-SY5Y cells (Wan et al. 2012). Reasonably, these several authors concluded that the decreased iron efflux reflected a reduction of plasma membrane Fpn abundance in the absence of APP although no direct evidence for a role for APP in iron efflux was provided in these studies. In contrast, we explicitly assessed the expression patterns of surface Fpn in APP RNAi-knockdown neurons. Significantly, even though APP expression was reduced by 80%, there was no change in the abundance of surface-localized Fpn. In addition, an increase of surface Hp was observed when APP was significantly reduced. Given that the surface expression of Fpn and Hp was not significantly altered by the absence of APP, it was not surprising that neither iron retention nor iron efflux was affected. Note that maturing primary hippocampal neurons (D15) were used in our assays, which differs from the previous studies using either immortalized neuronal cell lines (Duce et al. 2010; Wan et al. 2012) or immature primary neurons (D7) (Duce et al. 2010). In our study, we have shown that Hp expression is abundant in D15 neurons and that a significant amount of Hp is localized at the cell surface. Overall, our results indicate that APP is dispensable with respect to Fpn-mediated iron efflux in mature hippocampal neurons. In this context, iron accumulation in aged APP knockout animals (Needham et al. 2014) might result from some unknown function of APP which is associated with neuronal iron homeostasis, but not recapitulated in a D15 in vitro neuronal culture. Another possibility may attribute this difference to a species-specific difference in APP function, e.g., APP expressed in rat primary hippocampal neurons used in this study may vary from those in

mouse neurons. Despite the fact that the neuronal-specific isoform of APP protein found in rat and mouse share 99.7% identity in sequence, we acknowledge that species-specific differences may exist. On the other hand, the sequence of the APP motif that is associated with the stabilization of Fpn in the plasma membrane, a 22-amino acid sequence identified as the ferroportin targeting peptide, is 100% conserved in all archived mammalian genomes (McCarthy et al. 2014).

Hp mediates electron transfer from four molecules of ferrous iron to one dioxygen (Vashchenko and Macgillivray 2012). Hp and other multicopper oxidases (MCO), e.g., Cp, are also able to mediate oxidation of organic substrates, such as *p*-phenylenediamine and *o*-dianisidine (Vashchenko et al. 2011). Hp activity in cell lysates can be measured by the in-gel *p*-phenylenediamine assay. Previous in vitro (Nittis and Gitlin 2004; Chen et al. 2006; De Domenico et al. 2007; Chen et al. 2010; McCarthy and Kosman 2013) and in vivo studies (Chen et al. 2006; Broderius et al. 2010) have demonstrated that Cu restriction, typically established by treatment with a Cu-chelator, decreases the level of Hp, Cp, and/or Zp, and thus a reduction of cell (ferro)oxidase activity. Other studies have shown that a decrease in intracellular copper concentration or bioavailability does not affect Cp or Hp protein synthesis (Gitlin et al. 1992; Broderius et al. 2010; Mostad and Prohaska 2011), but dramatically enhanced the turnover rate of the mature but Cu-depleted protein (Nittis and Gitlin 2004). In the absence of a ferroxidase, surface Fpn is unstable corresponding to a fast rate of turnover (De Domenico et al. 2007; McCarthy and Kosman 2014, 2013; McCarthy et al. 2014). Studies also indicate that the ferroxidase activity of an MCO is required for surface Fpn stability (De Domenico et al. 2007; McCarthy and Kosman 2013). In the primary hippocampal neurons employed in this work, copper depletion by TTM and BCS lowered cell ferroxidase activity. BCS is a cell-impermeable copper chelator and thus restricts extracellular copper uptake in neurons. TTM is cell permeable and thus can chelate intracellular “labile” copper and form a stable complex with protein-bound copper. In these studies, BCS and TTM treatment appeared to be synergistic with respect to lowering the intracellular copper concentration and availability. Inhibition of ferroxidase activity by the copper chelators TTM and BCS correlated with a decreased surface Fpn abundance; in contrast, no change of the surface Hp or APP abundance was observed in these TTM/BCS-treated neurons. This could reflect the possibility that TTM was bound to the endogenous Hp and thereby influenced retrograde trafficking of Hp from the plasma membrane. Nevertheless, the decrease of surface Fpn in the TTM/BCS-treated neurons correlated with increased iron retention and decreased iron efflux, a result consistent with the importance of surface Fpn in iron efflux. Moreover, the data suggest that inhibition of Hp ferroxidase activity directly affects the rate of iron efflux; this inhibition appears to be relieved by sCp in as much as this exogenously added ferroxidase-reduced iron accumulation in the TTM/BCS-treated cultures.

Neuronal ferroxidase activity and iron efflux require functional Hp; this inference provides another example of the link between copper and iron metabolism. Decreased copper along with increased iron content has been observed in the substantia nigra of Parkinson’s disease patients (Dexter et al. 1989; Riederer et al. 1989; Dexter et al. 1991). As a result, ferroxidase activity in cerebrospinal fluid is reduced in Parkinson’s disease brains compared to healthy controls (Ayton et al. 2013; Olivieri et al. 2011; Boll et al. 1999). In Alzheimer’s disease,

intracellular copper deficiency as a result of extracellular amyloid β sequestration (Deibel et al. 1996) contributes to a regional decrease of ferroxidase Cp in the brain (Connor et al. 1993). Our data indicate that intracellular copper status also may play an autonomous role in modulating neuronal iron export through the Hp expressed by these neurons. The decrease in ferroxidase activity may enhance iron accumulation and result in an increase in oxidative stress in the affected cells (Prohaska 2011; Olivieri et al. 2011).

In conclusion, our results illuminate the molecular processes that support iron efflux in primary hippocampal neurons. We have demonstrated the expression and activity of neuronal Hp; the data indicate that Hp contributes to the stability of surface Fpn and to Fpn-mediated iron efflux. In contrast, our results indicate that APP plays at best an auxiliary role in support of neuronal iron efflux. Last, bioactive copper is required for neuronal Hp function in support of iron efflux, illustrating in neurons the interrelationship between iron and copper homeostasis.

## Supplementary Material

Refer to Web version on PubMed Central for supplementary material.

## Acknowledgments

This work was supported by Grants DK053820 and NS095063 from the National Institutes of Health to DJK.

## References

Abboud S, Haile DJ. A novel mammalian iron-regulated protein involved in intracellular iron metabolism. J Biol Chem. 2000; 275(26):19906–19912. https://doi.org/10.1074/jbc.M000713200. [PubMed: 10747949]

Aguirre P, Mena N, Tapia V, Arredondo M, Núñez M. Iron homeostasis in neuronal cells: a role for IREG1. BMC Neurosci. 2005; 6(1):1–11. https://doi.org/10.1186/1471-2202-6-3. [PubMed: 15649316]

Altamura S, Muckenthaler MU. Iron toxicity in diseases of aging: Alzheimer's disease, Parkinson's disease and atherosclerosis. J Alzheimers Dis. 2009; 16(4):879–895. https://doi.org/10.3233/JAD-2009-1010. [PubMed: 19387120]

Apelt J, Schliebs R, Beck M, Rossner S, Bigl V. Expression of amyloid precursor protein mRNA isoforms in rat brain is differentially regulated during postnatal maturation and by cholinergic activity. Int J Dev Neurosci. 1997; 15(1):95–112. [PubMed: 9099621]

Ayton S, Lei P, Duce JA, Wong BX, Sedjahtera A, Adlard PA, Bush AI, Finkelstein DI. Ceruloplasmin dysfunction and therapeutic potential for Parkinson disease. Ann Neurol. 2013; 73(4):554–559. https://doi.org/10.1002/ana.23817. [PubMed: 23424051]

Baj G, Patrizio A, Montalbano A, Sciancalepore M, Tongiorgi E. Developmental and maintenance defects in Rett syndrome neurons identified by a new mouse staging system in vitro. Front Cell Neurosci. 2014; 8:18. https://doi.org/10.3389/fncel.2014.00018. [PubMed: 24550777]

Barbariga M, Curnis F, Andolfo A, Zanardi A, Lazzaro M, Conti A, Magnani G, Volontè MA, Ferrari L, Comi G, Corti A, Alessio M. Ceruloplasmin functional changes in Parkinson's disease-cerebrospinal fluid. Mol Neurodegener. 2015; 10:59. https://doi.org/10.1186/s13024-015-0055-2. [PubMed: 26537957]

Beaudoin GM 3rd, Lee SH, Singh D, Yuan Y, Ng YG, Reichardt LF, Arikkath J. Culturing pyramidal neurons from the early postnatal mouse hippocampus and cortex. Nat Protoc. 2012; 7(9):1741–1754. https://doi.org/10.1038/nprot.2012.099. [PubMed: 22936216]

Boll MC, Sotelo J, Otero E, Alcaraz-Zubeldia M, Rios C. Reduced ferroxidase activity in the cerebrospinal fluid from patients with Parkinson's disease. Neurosci Lett. 1999; 265(3):155–158. [PubMed: 10327154]

Boserup MW, Lichota J, Haile D, Moos T. Heterogenous distribution of ferroportin-containing neurons in mouse brain. Biometals. 2011; 24(2):357–375. https://doi.org/10.1007/s10534-010-9405-2. [PubMed: 21213119]

Breton AB, Fox JA, Brownson MP, McEchron MD. Postnatal nutritional iron deficiency impairs dopaminergic-mediated synaptic plasticity in the CA1 area of the hippocampus. Nutr Neurosci. 2015; 18(6):241–247. https://doi.org/10.1179/1476830514y.0000000121. [PubMed: 24678581]

Broderius M, Mostad E, Wendroth K, Prohaska JR. Levels of plasma ceruloplasmin protein are markedly lower following dietary copper deficiency in rodents. Comp Biochem Physiol C: Toxicol Pharmacol. 2010; 151(4):473–479. [PubMed: 20170749]

Chen H, Attieh ZK, Su T, Syed BA, Gao H, Alaeddine RM, Fox TC, Usta J, Naylor CE, Evans RW, McKie AT, Anderson GJ, Vulpe CD. Hephaestin is a ferroxidase that maintains partial activity in sex-linked anemia mice. Blood. 2004; 103(10):3933–3939. https://doi.org/10.1182/blood-2003-09-3139. [PubMed: 14751926]

Chen H, Huang G, Su T, Gao H, Attieh ZK, McKie AT, Anderson GJ, Vulpe CD. Decreased hephaestin activity in the intestine of copper-deficient mice causes systemic iron deficiency. J Nutr. 2006; 136(5):1236–1241. [PubMed: 16614410]

Chen H, Attieh ZK, Syed BA, Kuo YM, Stevens V, Fuqua BK, Andersen HS, Naylor CE, Evans RW, Gambling L, Danzeisen R, Bacouri-Haidar M, Usta J, Vulpe CD, McArdle HJ. Identification of zyklopen, a new member of the vertebrate multicopper ferroxidase family, and characterization in rodents and human cells. J Nutr. 2010; 140(10):1728–1735. https://doi.org/10.3945/jn.109.117531. [PubMed: 20685892]

Chidambaram MV, Barnes G, Frieden E. Inhibition of ceruloplasmin and other copper oxidases by thiomolybdate. J Inorg Biochem. 1984; 22(4):231–240. [PubMed: 6097647]

Connor JR, Tucker P, Johnson M, Snyder B. Ceruloplasmin levels in the human superior temporal gyrus in aging and Alzheimer's disease. Neurosci Lett. 1993; 159(1–2):88–90. https://doi.org/10.1016/0304-3940(93)90805-U. [PubMed: 8264985]

De Domenico I, Ward DM, di Patti MC, Jeong SY, David S, Musci G, Kaplan J. Ferroxidase activity is required for the stability of cell surface ferroportin in cells expressing GPI-ceruloplasmin. EMBO J. 2007; 26(12):2823–2831. https://doi.org/10.1038/sj.emboj.7601735. [PubMed: 17541408]

Deibel MA, Ehmann WD, Markesbery WR. Copper, iron, and zinc imbalances in severely degenerated brain regions in Alzheimer's disease: possible relation to oxidative stress. J Neurol Sci. 1996; 143(1–2):137–142. [PubMed: 8981312]

Dexter DT, Wells FR, Agid F, Agid Y, Lees AJ, Jenner P, Marsden CD. Increased nigral iron content in postmortem parkinsonian brain. Lancet. 1987; 2(8569):1219–1220. [PubMed: 2890848]

Dexter DT, Wells FR, Lees AJ, Agid F, Agid Y, Jenner P, Marsden CD. Increased nigral iron content and alterations in other metal ions occurring in brain in Parkinson's disease. J Neurochem. 1989; 52(6):1830–1836. [PubMed: 2723638]

Dexter DT, Carayon A, Javoy-Agid F, Agid Y, Wells FR, Daniel SE, Lees AJ, Jenner P, Marsden CD. Alterations in the levels of iron, ferritin and other trace metals in Parkinson's disease and other neurodegenerative diseases affecting the basal ganglia. Brain. 1991; 114(Pt 4):1953–1975. [PubMed: 1832073]

Duce JA, Tsatsanis A, Cater MA, James SA, Robb E, Wikhe K, Leong SL, Perez K, Johanssen T, Greenough MA, Cho HH, Galatis D, Moir RD, Masters CL, McLean C, Tanzi RE, Cappai R, Barnham KJ, Ciccotosto GD, Rogers JT, Bush AI. Iron-export ferroxidase activity of beta-amyloid precursor protein is inhibited by zinc in Alzheimer's disease. Cell. 2010; 142(6):857–867. https://doi.org/10.1016/j.cell.2010.08.014. [PubMed: 20817278]

Ghadery C, Pirpamer L, Hofer E, Langkammer C, Petrovic K, Loitfelder M, Schwingenschuh P, Seiler S, Duering M, Jouvent E, Schmidt H, Fazekas F, Mangin JF, Chabriat H, Dichgans M, Ropele S, Schmidt R. R2* mapping for brain iron: associations with cognition in normal aging. Neurobiol Aging. 2015; 36(2):925–932. https://doi.org/10.1016/j.neurobiolaging.2014.09.013. [PubMed: 25443291]

Gitlin JD, Schroeder JJ, Lee-Ambrose LM, Cousins RJ. Mechanisms of caeruloplasmin biosynthesis in normal and copper-deficient rats. Biochem J. 1992; 282(Pt 3):835–839. [PubMed: 1554368]

Greminger AR, Lee DL, Shrager P, Mayer-Proschel M. Gestational iron deficiency differentially alters the structure and function of white and gray matter brain regions of developing rats. J Nutr. 2014; 144(7):1058–1066. https://doi.org/10.3945/jn.113.187732. [PubMed: 24744313]

Honarmand Ebrahimi K, Dienemann C, Hoefgen S, Than ME, Hagedoorn PL, Hagen WR. The amyloid precursor protein (APP) does not have a ferroxidase site in its E2 domain. PLoS ONE. 2013; 8(8):e72177. https://doi.org/10.1371/journal.pone.0072177. [PubMed: 23977245]

Jeong SY, David S. Glycosylphosphatidylinositol-anchored ceruloplasmin is required for iron efflux from cells in the central nervous system. J Biol Chem. 2003; 278(29):27144–27148. https://doi.org/10.1074/jbc.M301988200. [PubMed: 12743117]

Jeong SY, David S. Age-related changes in iron homeostasis and cell death in the cerebellum of ceruloplasmin-deficient mice. J Neurosci. 2006; 26(38):9810–9819. https://doi.org/10.1523/jneurosci.2922-06.2006. [PubMed: 16988052]

Ji C, Kosman DJ. Molecular mechanisms of non-transferrin-bound and transferring-bound iron uptake in primary hippocampal neurons. J Neurochem. 2015; 133(5):668–683. https://doi.org/10.1111/jnc.13040. [PubMed: 25649872]

Jiang, R., Hua, C., Wan, Y., Jiang, B., Hu, H., Zheng, J., Fuqua, BK., Dunaief, JL., Anderson, GJ., David, S., Vulpe, CD., Chen, H. Hephaestin and ceruloplasmin play distinct but interrelated roles in iron homeostasis in mouse brain. J Nutr. 2015. https://doi.org/10.3945/jn.114.207316

Lei P, Ayton S, Finkelstein DI, Spoerri L, Ciccotosto GD, Wright DK, Wong BX, Adlard PA, Cherny RA, Lam LQ, Roberts BR, Volitakis I, Egan GF, McLean CA, Cappai R, Duce JA, Bush AI. Tau deficiency induces parkinsonism with dementia by impairing APP-mediated iron export. Nat Med. 2012; 18(2):291–295. https://doi.org/10.1038/nm.2613. [PubMed: 22286308]

Matak P, Matak A, Moustafa S, Aryal DK, Benner EJ, Wetsel W, Andrews NC. Disrupted iron homeostasis causes dopaminergic neurodegeneration in mice. Proc Natl Acad Sci USA. 2016; 113(13):3428–3435. https://doi.org/10.1073/pnas.1519473113. [PubMed: 26929359]

McCarthy RC, Kosman DJ. Ferroportin and exocytoplasmic ferroxidase activity are required for brain microvascular endothelial cell iron efflux. J Biol Chem. 2013; 288(24):17932–17940. https://doi.org/10.1074/jbc.M113.455428. [PubMed: 23640881]

McCarthy RC, Kosman DJ. Glial cell ceruloplasmin and hepcidin differentially regulate iron efflux from brain microvascular endothelial cells. PLoS ONE. 2014; 9(2):e89003. https://doi.org/10.1371/journal.pone.0089003. [PubMed: 24533165]

McCarthy RC, Park YH, Kosman DJ. sAPP modulates iron efflux from brain microvascular endothelial cells by stabilizing the ferrous iron exporter ferroportin. EMBO Rep. 2014; 15(7):809–815. https://doi.org/10.15252/embr.201338064. [PubMed: 24867889]

Melgari JM, Marano M, Quattrocchi CC, Piperno A, Arosio C, Frontali M, Nuovo S, Siotto M, Salomone G, Altavilla R, di Biase L, Scrascia F, Squitti R, Vernieri F. Movement disorders and brain iron overload in a new subtype of aceruloplasminemia. Parkinsonism Relat Disord. 2015; 21(6):658–660. https://doi.org/10.1016/j.parkreldis.2015.03.014. [PubMed: 25864092]

Moos T, Rosengren Nielsen T. Ferroportin in the postnatal rat brain: implications for axonal transport and neuronal export of iron. Semin Pediatr Neurol. 2006; 13(3):149–157. https://doi.org/10.1016/j.spen.2006.08.003. [PubMed: 17101453]

Mostad EJ, Prohaska JR. Glycosylphosphatidylinositol-linked ceruloplasmin is expressed in multiple rodent organs and is lower following dietary copper deficiency. Exp Biol Med. 2011; 236(3):298–308. https://doi.org/10.1258/ebm.2010.010256.

Needham BE, Ciccotosto GD, Cappai R. Combined deletions of amyloid precursor protein and amyloid precursor-like protein 2 reveal different effects on mouse brain metal homeostasis. Metallomics. 2014; 6(3):598–603. https://doi.org/10.1039/c3mt00358b. [PubMed: 24448592]

Nittis T, Gitlin JD. Role of copper in the proteosome-mediated degradation of the multicopper oxidase hephaestin. J Biol Chem. 2004; 279(24):25696–25702. https://doi.org/10.1074/jbc.M401151200. [PubMed: 15087449]

Olivieri S, Conti A, Iannaccone S, Cannistraci CV, Campanella A, Barbariga M, Codazzi F, Pelizzoni I, Magnani G, Pesca M, Franciotta D, Cappa SF, Alessio M. Ceruloplasmin oxidation, a feature of

Parkinson's disease CSF, inhibits ferroxidase activity and promotes cellular iron retention. J Neurosci. 2011; 31(50):18568–18577. https://doi.org/10.1523/jneurosci.3768-11.2011. [PubMed: 22171055]

Prohaska JR. Impact of copper limitation on expression and function of multicopper oxidases (ferroxidases). Adv Nutr. 2011; 2(2):89–95. https://doi.org/10.3945/an.110.000208. [PubMed: 22332037]

Qian ZM, Chang YZ, Zhu L, Yang L, Du JR, Ho KP, Wang Q, Li LZ, Wang CY, Ge X, Jing NL, Li L, Ke Y. Development and iron-dependent expression of hephaestin in different brain regions of rats. J Cell Biochem. 2007; 102(5):1225–1233. https://doi.org/10.1002/jcb.21352. [PubMed: 17516501]

Riederer P, Sofic E, Rausch WD, Schmidt B, Reynolds GP, Jellinger K, Youdim MB. Transition metals, ferritin, glutathione, and ascorbic acid in parkinsonian brains. J Neurochem. 1989; 52(2): 515–520. [PubMed: 2911028]

Schulz K, Vulpe CD, Harris LZ, David S. Iron efflux from oligodendrocytes is differentially regulated in gray and white matter. J Neurosci. 2011; 31(37):13301–13311. https://doi.org/10.1523/jneurosci.2838-11.2011. [PubMed: 21917813]

Smith MA, Harris PL, Sayre LM, Perry G. Iron accumulation in Alzheimer disease is a source of redox-generated free radicals. Proc Natl Acad Sci USA. 1997; 94(18):9866–9868. [PubMed: 9275217]

Song N, Wang J, Jiang H, Xie J. Ferroportin 1 and hephaestin overexpression attenuate iron-induced oxidative stress in MES23.5 dopaminergic cells. J Cell Biochem. 2010a; 110(5):1063–1072. https://doi.org/10.1002/jcb.22617. [PubMed: 20564203]

Song N, Wang J, Jiang H, Xie JX. Ferroportin 1 but not hephaestin contributes to iron accumulation in a cell model of Parkinson's disease. Free Radic Biol Med. 2010b; 48(2):332–341. https://doi.org/10.1016/j.freeradbiomed.2009.11.004. [PubMed: 19913091]

Vashchenko G, Macgillivray RT. Functional role of the putative iron ligands in the ferroxidase activity of recombinant human hephaestin. J Biol Inorg Chem. 2012; 17(8):1187–1195. https://doi.org/10.1007/s00775-012-0932-x. [PubMed: 22961397]

Vashchenko G, Bleackley MR, Griffiths TA, MacGillivray RT. Oxidation of organic and biogenic amines by recombinant human hephaestin expressed in Pichia pastoris. Arch Biochem Biophys. 2011; 514(1–2):50–56. https://doi.org/10.1016/j.abb.2011.07.010. [PubMed: 21802403]

Vroegindeweij LH, Boon AJ, Wilson JH, Langendonk JG. Aceruloplasminemia: neurodegeneration with brain iron accumulation (NBIA) associated with parkinsonism. J Inherit Metab Dis. 2015; 38(2):375–376. https://doi.org/10.1007/s10545-014-9793-5. [PubMed: 25413956]

Wan L, Nie G, Zhang J, Zhao B. Overexpression of human wild-type amyloid-beta protein precursor decreases the iron content and increases the oxidative stress of neuroblastoma SH-SY5Y cells. J Alzheimers Dis. 2012; 30(3):523–530. https://doi.org/10.3233/jad-2012-111169. [PubMed: 22451308]

Wang J, Jiang H, Xie JX. Ferroportin1 and hephaestin are involved in the nigral iron accumulation of 6-OHDA-lesioned rats. Eur J Neurosci. 2007; 25(9):2766–2772. https://doi.org/10.1111/j.1460-9568.2007.05515.x. [PubMed: 17561842]

Wolkow N, Song D, Song Y, Chu S, Hadziahmetovic M, Lee JC, Iacovelli J, Grieco S, Dunaief JL. Ferroxidase hephaestin's cell-autonomous role in the retinal pigment epithelium. Am J Pathol. 2012; 180(4):1614–1624. https://doi.org/10.1016/j.ajpath.2011.12.041. [PubMed: 22342521]

Wong BX, Tsatsanis A, Lim LQ, Adlard PA, Bush AI, Duce JA. Beta-amyloid precursor protein does not possess ferroxidase activity but does stabilize the cell surface ferrous iron exporter ferroportin. PLoS ONE. 2014; 9(12):e114174. https://doi.org/10.1371/journal.pone.0114174. [PubMed: 25464026]

Wu LJ, Leenders AG, Cooperman S, Meyron-Holtz E, Smith S, Land W, Tsai RY, Berger UV, Sheng ZH, Rouault TA. Expression of the iron transporter ferroportin in synaptic vesicles and the blood-brain barrier. Brain Res. 2004; 1001(1–2):108–117. https://doi.org/10.1016/j.brainres.2003.10.066. [PubMed: 14972659]

Yeh K, Yeh M, Glass J. Interactions between ferroportin and hephaestin in rat enterocytes are reduced after iron ingestion. Gastroenterology. 2011; 141(1):292–299. e291. https://doi.org/10.1053/j.gastro.2011.03.059. [PubMed: 21473866]

Young-Pearse TL, Bai J, Chang R, Zheng JB, LoTurco JJ, Selkoe DJ. A critical function for beta-amyloid precursor protein in neuronal migration revealed by in utero RNA interference. J Neurosci. 2007; 27(52):14459–14469. https://doi.org/10.1523/jneurosci.4701-07.2007. [PubMed: 18160654]

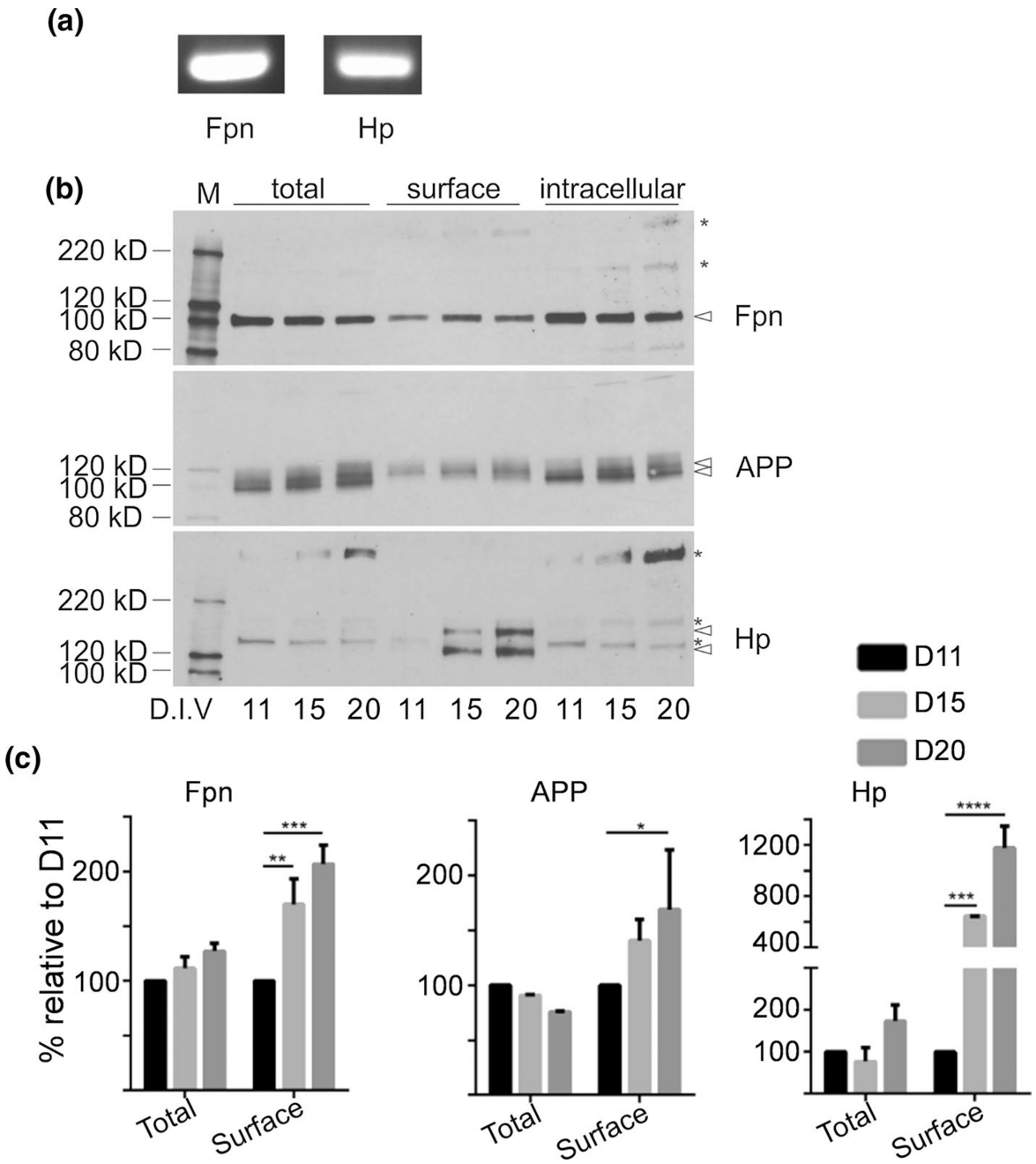


**Fig. 1.**

Ferroportin (Fpn), hephaestin (Hp), and amyloid precursor protein (APP) are expressed in rat primary hippocampal neurons. **a** Transcripts of Fpn and Hp. Total RNA was isolated from D11 primary hippocampal neurons, followed by one-step RT-PCR. The PCR product from the Fpn transcript was 357 bp; the Hp product was 516 bp. **b** Western blots of Fpn, APP, and Hp in rat hippocampal neurons cultured for 11, 15, or 20 days. Surface proteins were biotinylated and separated from the intracellular fraction. Samples loaded were total or intracellular protein (20 μg/per lane) and (per lane) the surface protein collected from 100 μg total protein sample. Arrow heads indicate the expected relative mass of each protein. Stars

indicate oligomer or post-translationally modified forms. **c** Quantification of western blots, based on two biologic replicates. Band intensities at D15 and D20 were normalized to D11. Statistical significance was tested by one-way ANOVA with Bonferroni's multiple comparisons test. *$p < 0.05$, **$p < 0.01$, ***$p < 0.001$; ****$p < 0.0001$

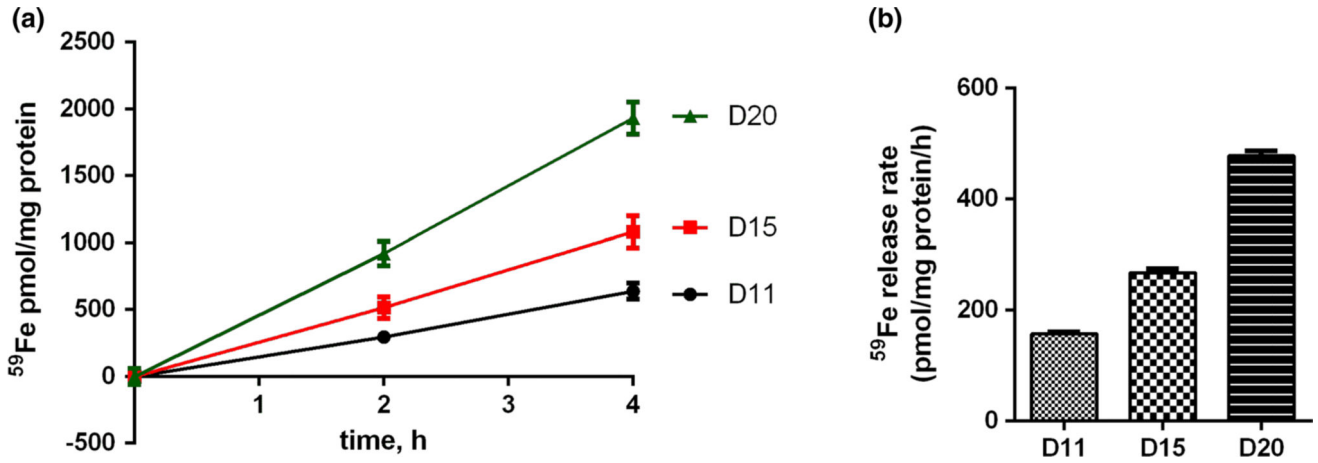


**Fig. 2.**

Developmental changes of Fe efflux in rat primary hippocampal neurons. **a** $^{59}$Fe efflux in primary hippocampal neurons grown for 11, 15, or 20 days. Neurons were incubated with 1 μM $^{59}$Fe-NTA for 16 h at 37 °C. The $^{59}$Fe-containing was removed and cells were washed with efflux medium containing 1 mM citrate. $^{59}$Fe efflux at 37 °C was then monitored by the appearance of radionuclide in the medium as a function of time. Six aliquots were quantified at each time point; duplicate experiments were performed. **b** The $^{59}$Fe-efflux rate as a function of neuronal development. The efflux data from (**a**) were analyzed by linear regression as represented by the connecting lines in (**a**). The $R^2$ values were D11, 0.9849; D15, 0.9866; and D20, 0.9691. The slopes of these fitted lines represent the velocity of $^{59}$Fe efflux; in (**b**) these values are plotted as function of days in culture

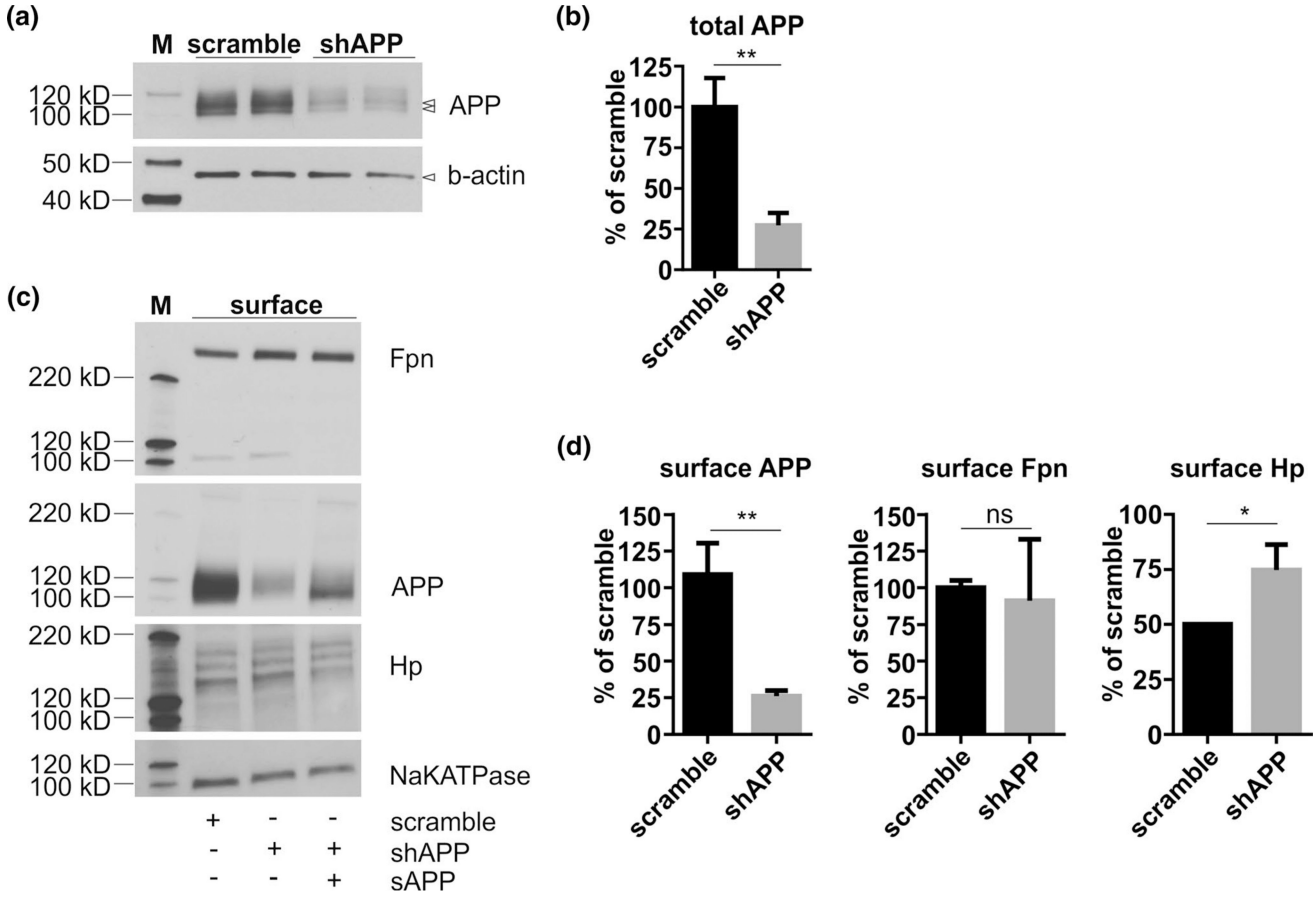


**Fig. 3.**

Endogenous APP plays a minor role in supporting surface Fpn localization in primary hippocampal neurons. **a** Western blot of APP in shRNA knockdown cells. Primary rat hippocampal neurons were infected by lentivirus containing scramble or APP knockdown shRNA. Lysates were isolated at 12 days after viral transduction. Band intensities were quantified as shown in (**b**); statistical significance was determined by unpaired t-test. $^{**}p < 0.01$. **c** Surface Fpn, APP, and Hp abundance in APP knockdown neurons. Primary neurons were treated as in (**a**), followed by surface biotinylation and western blotting. sAPPα (14 nM) was added to APP knockdown cultures for 24 h. **d** Quantification of western blots in (**c**) derived from triplicate biologic samples. Statistical significance was tested by unpaired t-test. $^{*}p < 0.05$; $^{**}p < 0.01$; ns, no significant difference

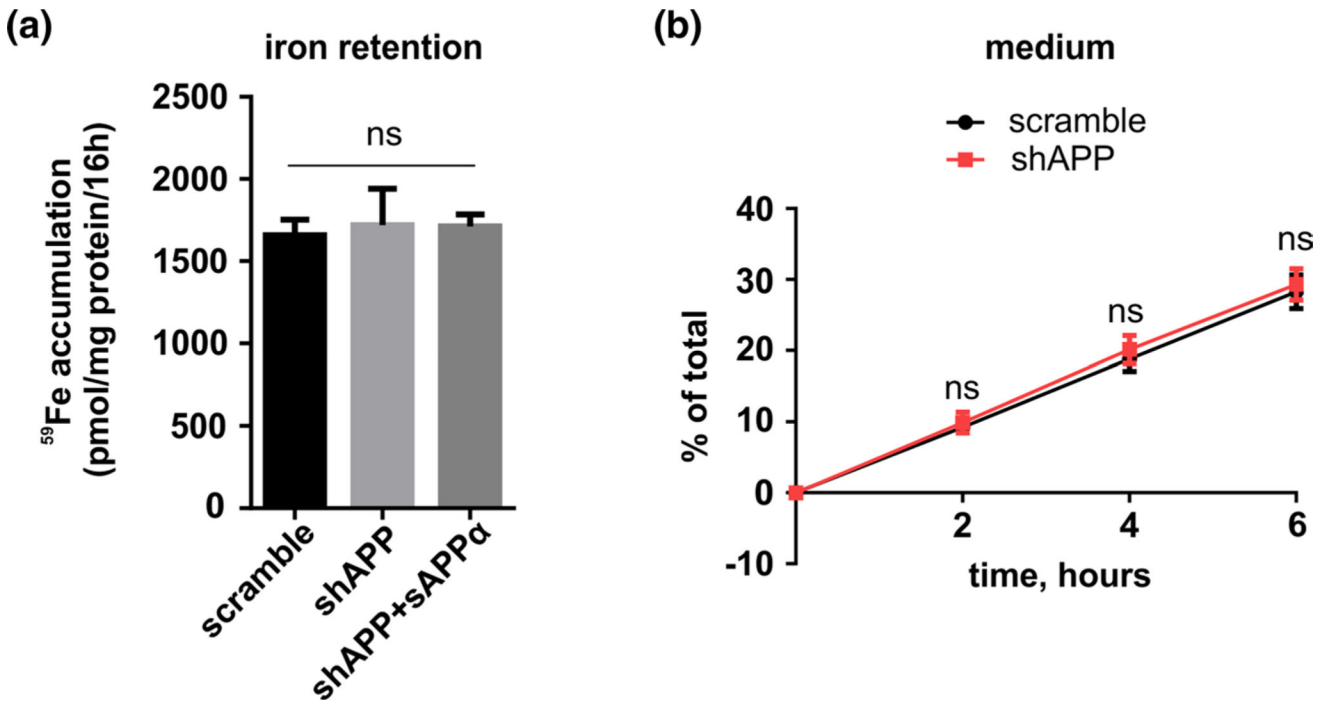


**Fig. 4.**

$^{59}$Fe accumulation does not change in the absence or presence of APP in primary hippocampal neurons. **a** $^{59}$Fe accumulation. Primary rat hippocampal neurons treated by either scramble or APP knockdown RNAi were incubated with 1 μM $^{59}$Fe-NTA for 16 h at 37 °C. One set of neurons with APP knockdown was loaded with $^{59}$Fe in the presence of 14 nM human sAPPα. Cell-associated $^{59}$Fe was quantified and normalized to the amount of total protein. Six replicates were included in each condition; experiments were repeated four times (biologic replicates). Statistical significance was tested by one-way ANOVA with Bonferroni's multiple comparisons test. ns, no significant difference. **b** $^{59}$Fe efflux in APP knockdown neurons. Neuronal cultures with either scramble or APP RNAi knockdown were loaded with 1 μM $^{59}$Fe-NTA for 16 h at 37 °C. Extracellular $^{59}$Fe was removed, the cultures were washed five times, and cells were then incubated in $^{59}$Fe-free medium. The percentage of $^{59}$Fe recovered in the medium over the initially accumulated $^{59}$Fe was quantified as a function of incubation time. Six replicates were included in each condition; experiments were repeated four times. Statistical significance was tested by two-way ANOVA with Sidak's multiple comparisons test. ns, no significant difference

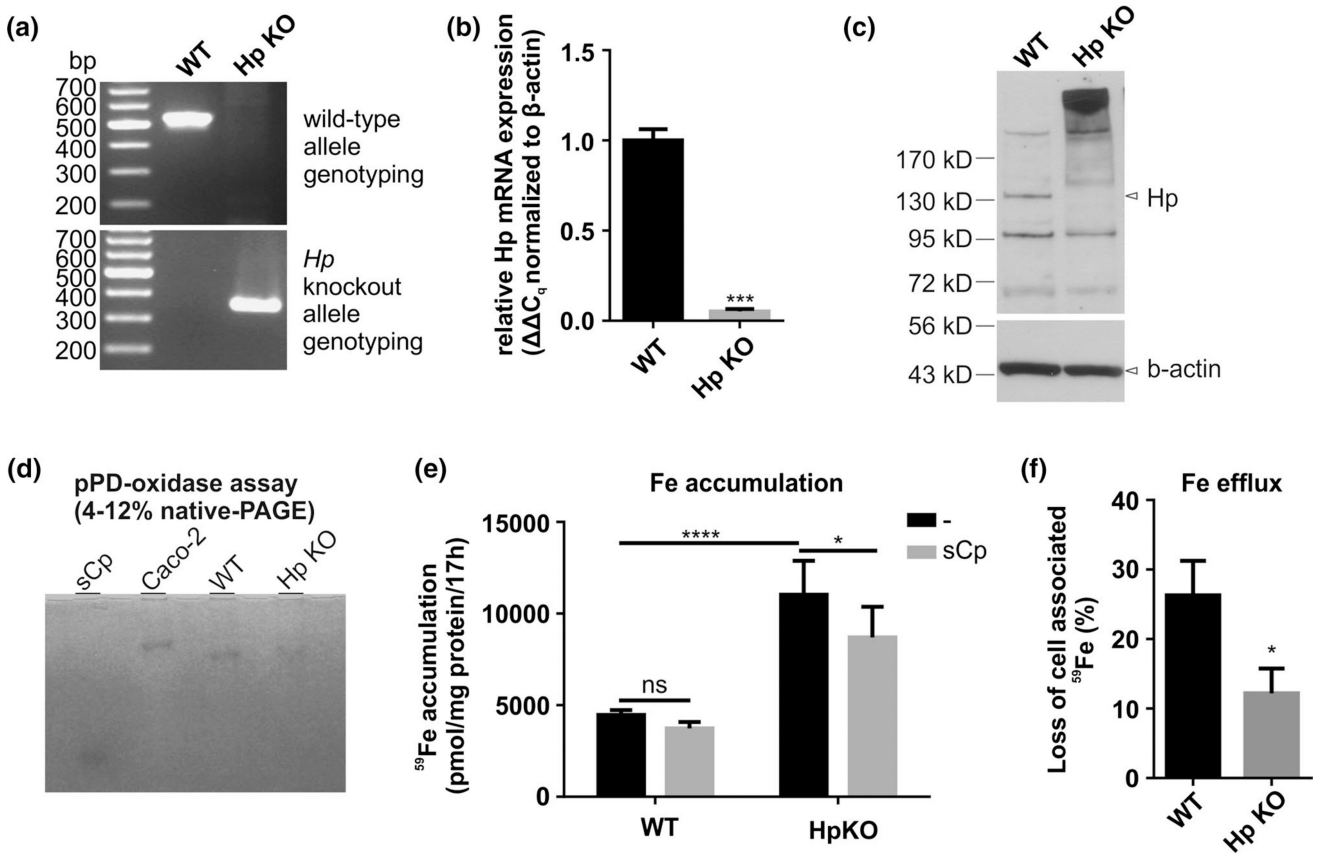


**Fig. 5.**

$^{59}$Fe efflux decreased in Hp knockout mouse hippocampal neurons. **a** Use of PCR to genotype neurons isolated from wild-type (564 bp) or *HEPH* knockout (363 bp) mice. **b** Quantitative RT-PCR for *HEPH* exon4 mRNA isolated from wild-type or *HEPH* knockout mouse neurons. Statistical significance was tested by unpaired t-test. ***$p < 0.001$. **c** Western blot of Hp in cultured hippocampal neurons isolated from wild-type or *HEPH* knockout mice. Arrow heads indicate Hp at the expected apparent molecular mass. **d** in-gel *p*-phenylenediamine (*p*PD) assay. Neuronal and Caco-2 lysates (80 μg total protein) were resolved in 4–12% native-PAGE. Human sCp (2 μg) was used as a positive control. The purple oxidized product was visible in the gel for sCp and the wild-type neuronal and Caco-2 lysates, and significantly reduced in the lysate prepared from *HEPH* knockout neurons. **d** *HEPH* knockout neurons accumulated more $^{59}$Fe compared to wild-type neurons. Cells were loaded with $^{59}$Fe-NTA (1 μM) for 17 h in the absence or presence of 0.25 μM sCp and cell-associated $^{59}$Fe was quantified. Six replicates were used in each condition with data collected from duplicate biologic experiments. Statistical significance was tested by two-way ANOVA with Holm–Sidak's multiple comparisons test. *$p < 0.05$; ****$p < 0.0001$; ns, no significant difference. **e** $^{59}$Fe efflux in *HEPH* knockout neurons was reduced compared to wild-type neurons. Percent loss of total cell-associated $^{59}$Fe was used to represent $^{59}$Fe efflux. Statistical significance was tested by unpaired t-test. *$p < 0.05$. WT, wild-type mouse neurons; Hp KO, *HEPH* knockout mouse neurons

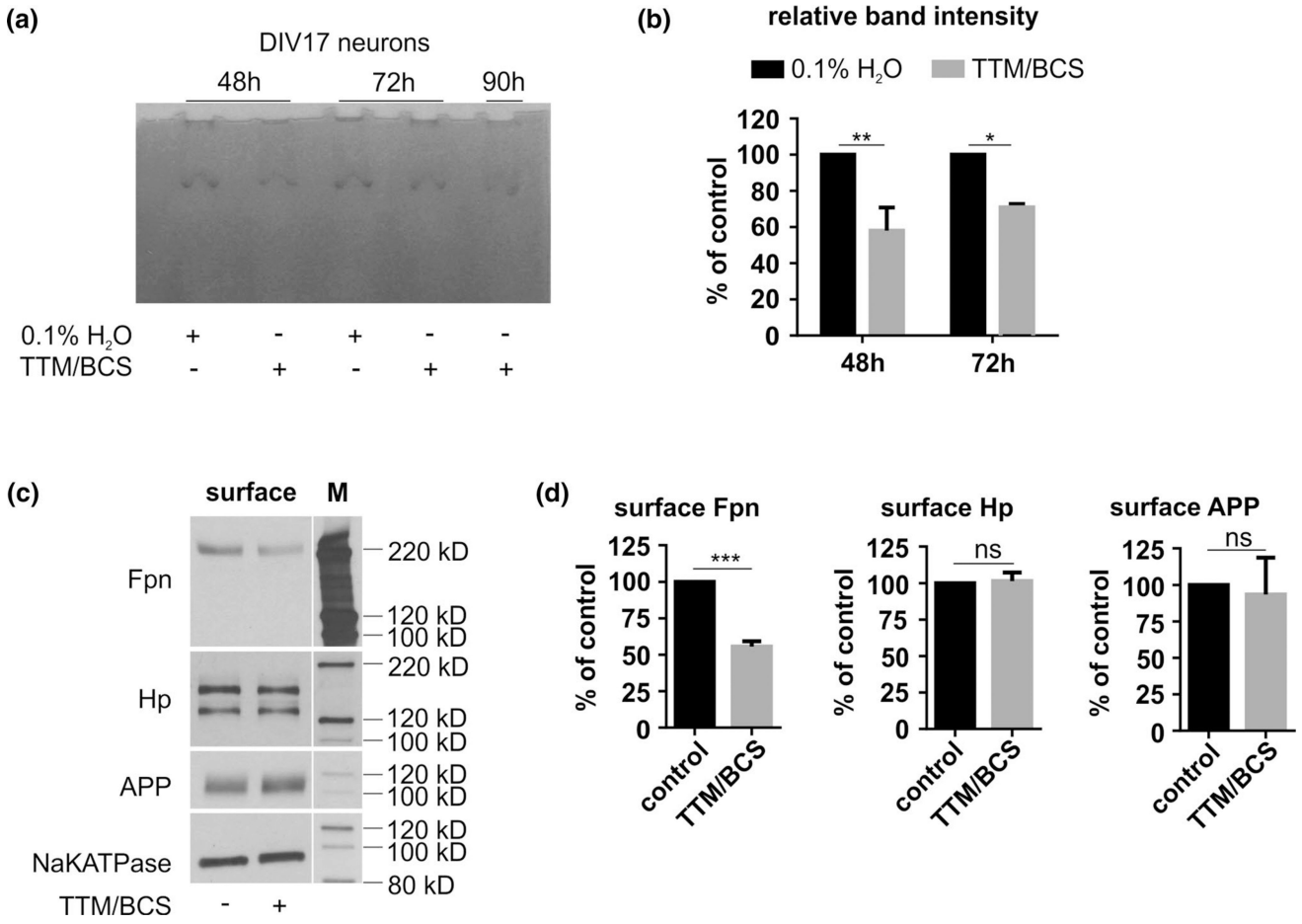


**Fig. 6.**

Cu restriction decreased neuronal (ferro)oxidase activity and surface Fpn abundance. **a** *p*PD oxidase activity decreased in neuronal lysates treated with ammonium tetrathiomolybdate (TTM) and bathocuproine disulfonate (BCS). Primary hippocampal neurons were treated with 0.1% $H_2O$ or 1 μM TTM and 200 μM BCS for 48 h, 72 h, or 90 h. Total neuronal lysates were isolated and resolved in 4–12% native-PAGE gels. **b** Quantification of relative band intensity in (**a**) based on triplicate experiments. Statistical significance was tested by unpaired t-test. $*p < 0.05$; $**p < 0.01$. **c** Surface Fpn, Hp, and APP abundance in primary hippocampal neurons after Cu restriction. Neurons were treated with 0.1% $H_2O$ or 1 μM TTM/200 μM BCS for 48 h, then surface protein was biotinylated and processed for western blots analysis. **d** Quantification of Fpn, Hp, and APP blots, based on triplicate experiments. Statistical significance was tested by unpaired t-test. $***p < 0.001$; ns, no significant difference

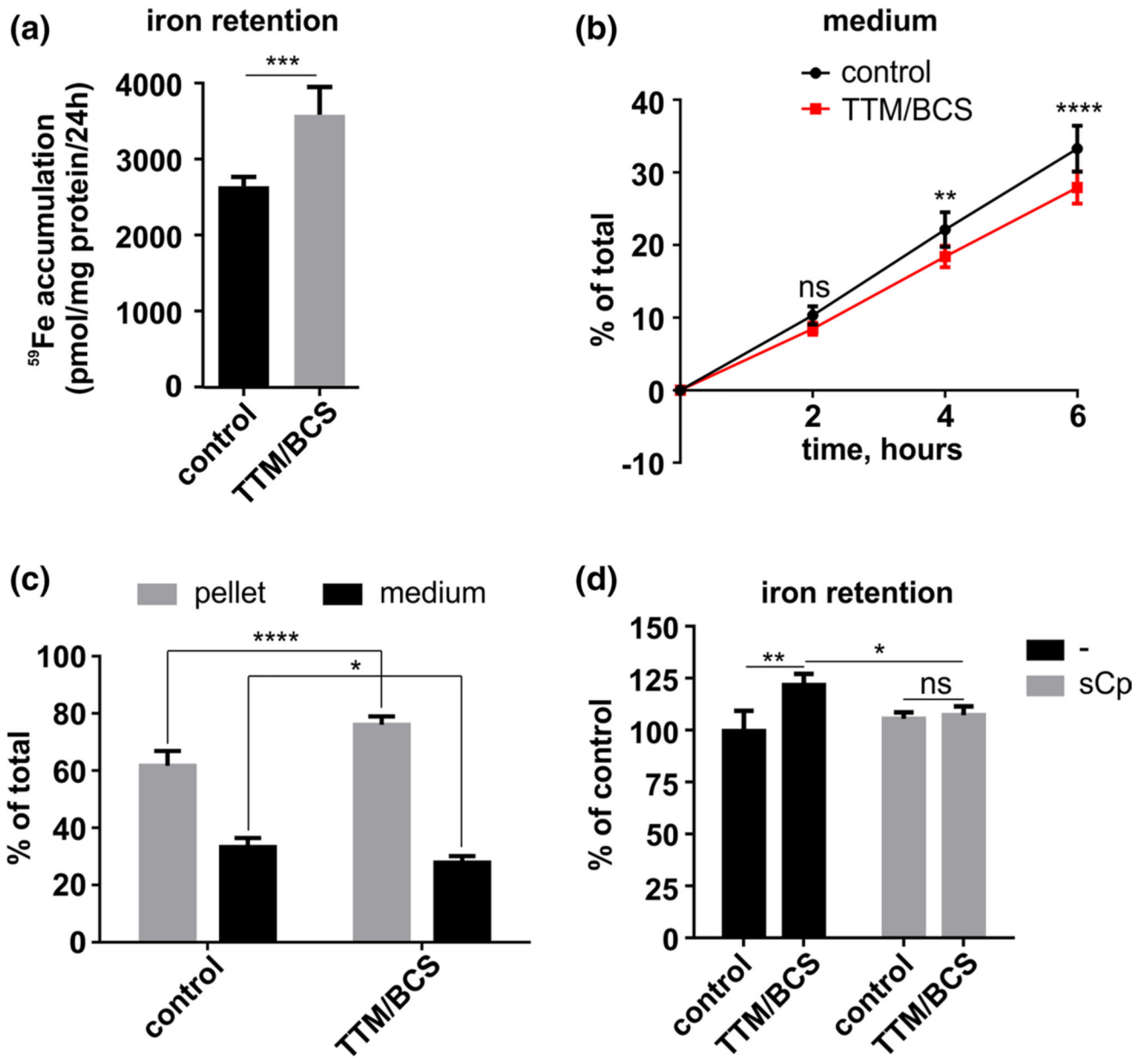


**Fig. 7.**

Cu restriction affects $^{59}$Fe accumulation and $^{59}$Fe efflux in primary hippocampal neurons. **a** $^{59}$Fe accumulation in neurons after Cu restriction. Neurons were treated with 1 μM TTM/200 μM BCS for 48 h. Control and TTM/BCS cultures were incubated with 1 μM $^{59}$Fe-NTA for 24 h; TTM/BCS remained in the latter cultures. Cell-associated $^{59}$Fe was quantified as described. Six replicates were used in each condition; experiments were repeated three times. Statistical significance of difference was quantified by unpaired t-test. ***$p < 0.001$. **b** $^{59}$Fe efflux in neurons after Cu restriction. Neurons were treated with TMM/BCS and loaded with 1 μM $^{59}$Fe-NTA as described in (**a**). After thorough washing, $^{59}$Fe efflux into fresh medium was monitored over time in the absence or presence of TTM/BCS. The percentage of $^{59}$Fe present in the medium relative to the total amount of $^{59}$Fe in the culture represented the fractional Fe efflux. Six replicates were included in each

condition; experiments were repeated twice. Statistical significance was tested by two-way ANOVA with Sidak's multiple comparisons test. $^{**}p < 0.01$; $^{****}p < 0.0001$; ns, no significant difference. **c** $^{59}$Fe distribution after TTM/BCS treatment. Cell-associated $^{59}$Fe was quantified after $^{59}$Fe efflux in (**b**). Total $^{59}$Fe was taken from the combination of cell-$^{59}$Fe and medium-associated $^{59}$Fe. The amount of each fraction relative to the total $^{59}$Fe was calculated for each condition. Statistical significance was tested by two-way ANOVA with Bonferroni's multiple comparisons test. $^{*}p < 0.05$. $^{****}p < 0.0001$. **d** Exogenous ferroxidase activity reduced $^{59}$Fe retention in Cu-restricted neurons. Neurons were treated without or with TTM/BCS for 48 h and then incubated with 1 μM $^{59}$Fe-NTA for 24 h in the absence or presence of 0.25 μM human sCp. Cell-associated $^{59}$Fe was quantified; the $^{59}$Fe-accumulation in the TTM/BCS-treated cultures (−/+sCp) is represented relative to the untreated control. Three replicates were included in each condition; experiments were repeated twice. Statistical significance was tested by two-way ANOVA with Bonferroni's multiple comparisons test. $^{*}p < 0.05$; $^{**}p < 0.01$; ns, no significant difference